Finite-time thermodynamics and the gas-liquid phase transition

M. Santoro,* J. C. Schön,† and M. Jansen‡
Max-Planck-Institut für Festkörperforschung, Heisenbergstrasse 1, D-70569 Stuttgart, Germany
(Received 19 March 2007; revised manuscript received 10 August 2007; published 20 December 2007)

In this paper, we study the application of the concept of finite-time thermodynamics to first-order phase transitions. As an example, we investigate the transition from the gaseous to the liquid state by modeling the liquification of the gas in a finite time. In particular, we introduce, state, and solve an optimal control problem in which we aim at achieving the gas-liquid first-order phase transition through supersaturation within a fixed time in an optimal fashion, in the sense that the work required to supersaturate the gas, called excess work, is minimized by controlling the appropriate thermodynamic parameters. The resulting set of coupled nonlinear differential equations is then solved for three systems, nitrogen N_2, oxygen O_2, and water vapor H_2O.

DOI: 10.1103/PhysRevE.76.061120 PACS number(s): 05.70.−a, 64.70.Fx, 02.30.Yy, 64.60.Qb

I. INTRODUCTION

Phase transitions are well-known phenomena in many area of physics, where the dynamics of complex systems leads to the existence of several (meta)stable phases as a function of characteristic parameters [1]. Typically, these transitions occur for a particular set of values of the characteristic parameters C_i, for which certain physical quantities Q_j of the two phases under consideration are equal. In thermodynamic systems, we often consider only one physical parameter Q, which corresponds to the (free) energy of the competing phases, while the C_i represent temperature, pressure, etc. For a given temperature and pressure, the phase with the lowest free energy is most likely to be present and is thus considered to be thermodynamically stable. This follows from the fact that classical thermodynamical processes are assumed to take place infinitely slowly, and thus equilibrium statistical mechanics can be applied to compute the probability that a certain phase is present. However, it is well known that, in real systems, where only a finite time is available for the phase transition to take place, a given phase can often persist for a considerable time even at temperatures and pressures where it has become thermodynamically unstable. This metastability of a phase is a common occurrence in cases of first-order phase transitions, where a nucleation process is necessary before a new phase is formed. Typical examples are the condensation of a liquid from the gas phase below the critical point, crystallization from the melt (where supercoolings of up to hundreds of degrees have been observed), and many among the temperature- or pressure-induced phase transitions in crystalline solids [2]. The physical reason behind this metastability is the existence of a slow dynamics, possibly driven by rare fluctuations, for the rearrangement of the individual atoms, spins, etc. Accelerating this dynamics usually can be achieved by moving from the phase boundary in parameter space deeper into the region of the new phase. As a consequence, the transition in finite time takes place under nonequilibrium conditions and dissipation occurs, reflected in, e.g., losses of availability or excess of entropy production. Such effects are well known in the theory of finite-time thermodynamics, where the consequences of running thermodynamic processes in finite time are being studied [3–7]. A question of particular interest is the derivation of lower bounds on the entropy production using optimal control techniques, since the knowledge of such limits and the precise schedule in thermodynamic parameters allows the design of optimally energy-efficient processes. Examples include efficient design of heat exchangers [8,9], distillation columns [10], and heat engines [11,12]; however, the issue of completing a first-order phase transition in a finite time and the associated question of how to drive the system in an optimal way such that the work spent in doing so is minimal does not seem to have been considered up to now.

Thus, in this work, we introduce, state, and solve the optimal control problem for achieving a first-order phase transition in an optimal fashion, in the sense that the excess work required is minimized by controlling the appropriate thermodynamic parameters. As a concrete example, we choose the transition from the gaseous to the liquid state, with the excess work corresponding to the work required to supersaturate the gas.

The focus of this work is on the application of the principles of finite-time thermodynamics to first-order phase transitions; thus we employ some simplifications in the description of the actual physical system, such as using classical nucleation theory when modeling the gas-liquid transition, that allow us to reduce the solution of the optimal control problem to a set of coupled ordinary differential equations that can be solved numerically.

II. MODEL

To mathematically formulate the problem of achieving a first-order phase transition in a finite time in an optimal fashion, we need a complete, clear, and simple description of a nucleation process and subsequent cluster growth in which the relevant physics is present but which nevertheless allows an efficient solution. For this, we turn to the well-known homogeneous classical nucleation theory (see Appendix A), which should be able to serve as a satisfactory basic description of the gas-liquid transition. Here, the supersaturated vapor phase is supposed to behave as an ideal gas of monomers without foreign seed particles, while the liquid phase appears

*M.Santoro@fkf.mpg.de
†C.Schoen@fkf.mpg.de
‡M.Jansen@fkf.mpg.de

via the growth of clusters by condensation of monomers. The liquid phase is supposed to be incompressible, and it is assumed that the clusters and the monomers have the same temperature [13]. Using this assumption, it is possible to obtain the steady state isothermal[1] rate of formation of stable particles of the new phase as a function of the bulk physical properties of the material, the temperature, and the degree of supersaturation of the system [13]. By assuming isothermal conditions, classical nucleation theory ignores any of the processes that could contribute to temperature differences between the old and the new phases, in particular any energy released or required by the phase transition. Following these guidelines, we define a molecular transfer rate from the gas to the liquid phase in which both a nucleation and a growth term are present, and we write down the excess work rate function, which is described by the $(p_g - p_g^\infty)dV$ work term along the pressure path $p_g(t)$ of the system. In other words, we want to investigate how we can push the system to overcome its energy barrier and, therefore, to liquefy, in a specific time interval, and how we can minimize the amount of work involved, starting at standard conditions $[p_g^\infty(T^{boil}), T^{boil}]$, where T^{boil} is the boiling temperature of the system at the pressure $p_g = p_g^\infty(T^{boil})$. For the sake of clarity, we make a distinction between the pressure of the system as a state parameter and the applied pressure as the control we want to optimize. Of course, applying the pressure to the system along isotherms forces the system to adjust to the new condition with a certain time lag. For simplicity, we shall assume that such an adjustment is immediate.

Consider the total volume of the system as the sum of the volumes of the gas and liquid phases, $V_T = V_g + V_l = n_g \nu_g + n_l \nu_l$, where $n_{g,l}$ and $\nu_{g,l}$ are the number of molecules and the molecular volume of the corresponding phase. Supposing constant molecular volume of the liquid (i.e., incompressibility of the liquid phase), we have

$$\frac{dV_T}{dt} = n_g \frac{d\nu_g}{dt} + (\nu_l - \nu_g)\frac{dn_l}{dt}, \tag{1}$$

since $dn_l/dt = -dn_g/dt$ by conservation of mass, $n_T = n_g + n_l = \text{const}$. Using $\nu_g = kT/p_g$, we now define the rate at which mass is transferred from the gaseous phase to the liquid phase as the sum of the rate at which nuclei are formed and the rate at which these nuclei grow,

$$\frac{dn_l}{dt} = n_l^c J_{ss}^c + \frac{(4\pi)^{1/3}(3\nu_l)^{2/3}}{\sqrt{2\pi mkT}} n_l^{2/3}(p_g - p_g^\infty)\left(\int_0^t J_{ss}^c dt'\right)^{1/3}, \tag{2}$$

with n_l^c given by Eq. (A3). On the right side, the first term is the nucleation term, which accounts for the net increase in the number of liquid droplets in the gas phase during the transition. The second term is the average growth term of clusters, which is essentially the difference between the forward and backward rates of molecules entering and leaving the clusters. Denoting the number of molecules in one cluster as n_l^1, the forward rate, i.e., the rate at which impinging molecules condense, is classically given, per cluster, by the product of the surface area $A(n_l^1) = (4\pi)^{1/3}(3\nu_l)^{2/3}(n_l^1)^{2/3}$, the impingement rate of molecules on the cluster $\beta = p_g/\sqrt{2\pi mkT}$, and the condensation coefficient which we assume to be unity [13,14]. The backward rate per cluster, on the other hand, while also depending on the surface area and on the condensation coefficient, takes into account the amount of mass leaving the cluster by considering the Kelvin equation, in which the partial pressure of the vapor is in equilibrium with a liquid droplet of size n_l^1. For simplicity, we assume that no molecule leaves the droplet as long as $p_g > p_g^\infty$ and, therefore, the rate of molecules leaving the cluster can be given by $p_g^\infty/\sqrt{2\pi mkT}$. Finally, the integral term in Eq. (2) takes into account the total number of critical clusters created during the process. For simplicity, we do not keep track of the growth of each cluster individually. Instead, we employ an average value $N^c = n_l/n_l^1$. This does not allow the treatment of coarsening processes; however, we note that such processes usually proceed rather slowly, while we are interested in the finite-time behavior of the phase transition.

The excess work rate is given by

$$\frac{dW_{exc}}{dt} = -(p_g - p_g^\infty)\frac{dV_T}{dt} = (p_g - p_g^\infty)\left[(n_T - n_l)\frac{kT}{p_g^2}\frac{dp_g}{dt} + \left(\frac{kT}{p_g} - \nu_l\right)\frac{dn_l}{dt}\right], \tag{3}$$

where we have used Eqs. (1) and (2). The excess work is the work we need to perform to achieve the transition at supersaturation, which is null if $p_g = p_g^\infty$, increases as a function of p_g/p_g^∞, and can be visualized by the shaded region in Fig. 1. Indeed, supppose that the system is in the gas phase at temperature T_1, standard pressure $p_g^\infty(T_1)$, and volume V_1. If we leave the system at these standard conditions, eventually a fluctuation big enough to overcome the energy barrier will allow liquification of the gas with no work done in the sense of Eq. (3). But, except for temperatures close to the critical point, such an event will require essentially an infinite time. Thus, in a finite-time regime, we need to assist the system to change from the gaseous to the liquid phase by applying an external pressure $p_a > p_g^\infty$ along isotherm T_1. This external help requires an additional amount of work, which is related just to the increment of the pressure from standard conditions such that a nucleating process, and subsequent growth of the clusters, can occur. Minimizing this excess work while moving the system from the gaseous to the liquid phase is equivalent to the following optimal control problem in the framework of finite-time thermodynamics and classical nucleation theory.

Given fixed initial and final times t_0 and t_f, we aim at achieving a complete first-order phase transition in an optimal fashion along isotherms by controlling the applied pressure $p_a(t)$ that will cause the system to go from the gaseous to the liquid phase in a finite time obeying Eq. (2) while minimizing the total excess work produced, i.e., $\int_{t_0}^{t_f}(dW_{exc}/dt)dt$.

[1]For an extension of the classical homogeneous nucleation theory to nonisothermal conditions, we refer to Ref. [22].

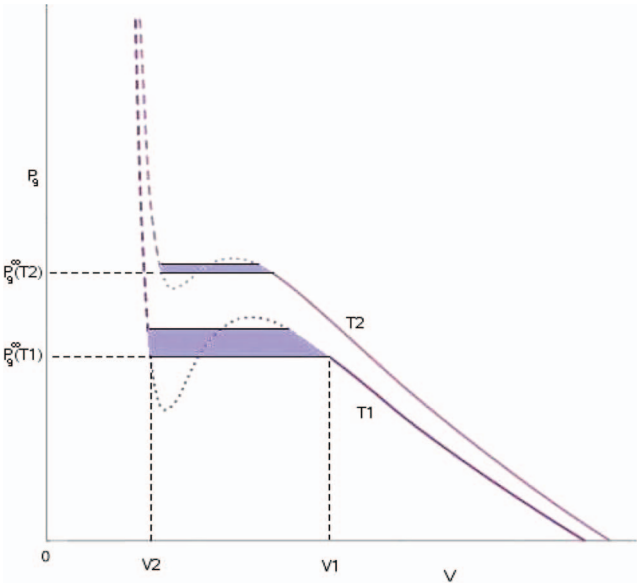

FIG. 1. (Color) The shaded region represents the work, called *excess work*, we need to perform to achieve a first-order phase transition by supersaturating the gas at standard conditions $[p_g^\infty(T^{boil}), T^{boil}]$, where T^{boil} is the boiling temperature of the system. Here, T^{boil} is either T_1 or T_2 depending on the system.

In the next section, we recast the physical problem in the formalism of optimal control theory, and derive the set of nonlinear differential equations and boundary conditions that yield the optimal trajectory $p_a^*(t)$. The general mathematical apparatus needed is outlined in Appendix B.

III. OPTIMAL CONTROL PROBLEM

A. Formulation as a calculus-of-variation problem

In the context of optimal control theory, the total excess work corresponds to expression (B1) from Appendix B. $\mathfrak{I}(\bar{\boldsymbol{x}}(t),\bar{\boldsymbol{u}}(t))$ corresponds to dW_{exc}/dt in Eq. (3) and the generalized coordinates and the generalized velocities are given by $\boldsymbol{x}(t)=(x_1(t),x_2(t))=(n_l(t),p_g(t))\in R^2$ and $\dot{\boldsymbol{x}}(t)=(\dot{x}_1(t),\dot{x}_2(t))=(\dot{n}_l(t),\dot{p}_g(t))\in R^2$, respectively. Moreover, the control variable $u(t)$, in Appendix B, is the externally applied pressure $p_a(t)$. For the purpose of this analysis, we assume that the delay of equilibration of the internal pressure p_g to the applied external pressure p_a is essentially zero,[2] i.e.,

$$p_g(t)=p_a(t) \tag{4}$$

for all $t\in[t_0,t_f]$. In terms of an optimal control problem, we need to define the admissible sets of state and control variables. Considering the general situation in which the initial and final number of molecules in the liquid phase are given by $n_l(t_0)$, not necessarily zero, and $n_l(t_f)$, not necessarily n_T, we choose the state variables to be given by the set $(n_l(t),p_g(t))\in X\subset R^2$, with $X=\{[n_l(t_0),n_l(t_f)]\times[p_g^\infty,\infty)\}$, and the control variables to be given by the set $(p_a(t),\dot{p}_a(t))\in U\subset R^2$, with $U=\{[p_g^\infty,\infty)\times(-\infty,\infty)\}$.[3] It is important to mention that the finite-time feature of our problem will restrict further the set U to exclude any admissible pressure path $p_a(t)$ which intersect the transition pressure p_g^∞ for any $t\in(t_0,t_f)$. Moreover, the applied pressure p_a has to be considered as both a state and a control variable, and the optimal number of molecules migrated from the gas to the liquid phase, n_l^*, will not take values on the boundary of X, except at the extreme points $n_l(t_0)$ and $n_l(t_f)$, due to the growth term in the ordinary differential equation (2). It is evident that we are seeking an optimal continuous change of the pressure such that a complete transition occurs in a finite time, and we also insist that the pressure rate $\dot{p}_g(t)$ change continuously for all $t\in(t_0,t_f)$. Based on this fact, we shall derive the necessary condition for optimality.

B. Necessary conditions of the physical problem

In defining our cost functional, we omit the state constraint vector value function (B4), since we can define such constraints in a simpler form in this problem. Moreover, the number of molecules is fixed at the fixed initial time t_0 and fixed final time t_f, namely, $n_l(t_0)=n_l^0$ and $n_l(t_f)=n_l^f$. Thus, considering that $\mathfrak{I}(\cdot)=(dW_{exc}/dt)(\cdot)$ and $\phi(p_a(t_0),p_a(t_f))=W_{exc}(p_a(t_0),p_a(t_f))$, we can restate problem (B3) as

$$\min\left[\phi(p_a(t_0),p_a(t_f))+\int_{t_0}^{t_f}\mathfrak{I}(n_l(t),p_a(t),\dot{p}_a(t),t)dt\right], \tag{5}$$

subject to

$$\dot{n}_l(t)=f(n_l(t),p_a(t),t)=n_l^c J_{ss}^c+\frac{(4\pi)^{1/3}(3\nu_l)^{2/3}}{\sqrt{2\pi mkT}}n_l^{2/3}(p_a-p_g^\infty)\times\left(\int_0^t J_{ss}^c dt'\right)^{1/3}, \tag{6}$$

$$\dot{p}_g(t)=\dot{p}_a(t) \tag{7}$$

with $n_l(t_0)=n_l^0$, $n_l(t_f)=n_l^f$, $p_a(t)\in[p_g^\infty,\infty)$, $\dot{p}_a(t)\in(-\infty,\infty)$, and with $\mathfrak{I}$ and f continuous for all $t\in[t_0,t_f]$ and continuously differentiable for all $t\in(t_0,t_f)$, given the admissible state and control region defined in the previous section. Now, the cost functional we are going to consider is given by [see (B6)],

[2] In general, we would also take into account the loss of availability that is due to the fact that only a finite time is available for the equilibration before p_a changes again. Similarly, one would also add finite-time dissipation terms due to the difficulty of keeping the temperature constant during the process. However, we will neglect such terms in our analysis, since they are expected to be relatively small compared to the excess work in Eq. (3).

[3] It has to be mentioned that, even though the sets of admissible applied pressures and applied pressure rates we consider, namely, $p_a(t)\in[p_g^\infty,\infty]$ and $\dot{p}_a(t)\in(-\infty,\infty)$, are in reality constrained by the physical limitations of the experimental tools available, the pressure and pressure rate values that can be obtained in a laboratory are so much greater than the one physically admissible in our problem that we should keep the pressure intervals as they are. In other words, the boundaries given by experimental performance of laboratory devices have no effect on our problem solutions.

TABLE I. Thermodynamic parameters for nitrogen, oxygen, and water vapor.

Parameters (units)	N_2	O_2	H_2O
Molar mass M (kg/mole)	0.028013 [15]	0.032	0.01801539
Molecular mass m (kg)	4.65175×10^{-26}	5.31372×10^{-26} [16]	2.99147×10^{-26}
Boiling point at p_g^∞, T^{boil} (K)	77.35 [15]	90.15 [16]	373.15 [17]
Density ρ (kg/m^3)	806.082 [15]	1142	958.356 [18]
Molecular volume v_l (m^3)	5.77081×10^{-29}	4.65299×10^{-29} [16]	3.12146×10^{-29}
Surface tension at T^{boil}, γ (N/m)	0.00885 [19]	0.0131 [16]	0.0606 [18]

$$J=\phi(p_a(t_0),p_a(t_f))+\int_{t_0}^{t_f}(\lambda_1\dot{n}_l+\lambda_2\dot{p}_a-H)dt, \tag{8}$$

in which the Hamiltonian H is given by [see (B5)],

$$H(n_l(t),p_a(t),\dot{p}_a(t),\lambda_1(t),\lambda_2(t),t)$$
$$=\lambda_1 f(n_l(t),p_a(t),t)+\lambda_2\dot{p}_a-\mathfrak{I}(n_l(t),p_a(t),\dot{p}_a(t),t). \tag{9}$$

We set the first variation of J to zero to obtain the necessary conditions for the optimal applied pressure trajectory $p_a^*(t)$. This yields, considering the cost in Eq. (8) and the fact that $\delta n_{l_f}=\delta n_{l_0}=\delta t_f=\delta t_0=0$,

$$\dot{n}_l^*=\frac{\partial H^*}{\partial\lambda_1}=\frac{\partial\tilde{H}^*}{\partial\lambda_1}, \tag{10}$$

$$\dot{p}_a^*=\frac{\partial H^*}{\partial\lambda_2}=\dot{p}_g^*, \tag{11}$$

$$\dot{\lambda}_1^*=-\frac{\partial H^*}{\partial n_l}=-\frac{\partial\tilde{H}^*}{\partial n_l}, \tag{12}$$

$$\dot{\lambda}_2^*=\frac{d}{dt}\left(\frac{\partial H^*}{\partial\dot{p}_a}\right)-\frac{\partial H^*}{\partial p_a}\Rightarrow\frac{d}{dt}\left(\frac{\partial\tilde{H}^*}{\partial\dot{p}_a}\right)-\frac{\partial\tilde{H}^*}{\partial p_a}=0, \tag{13}$$

where $H^*=H(n_l^*,p_a^*,\lambda_1^*,\lambda_2^*,t)$ and $\tilde{H}^*=\tilde{H}(n_l^*,p_a^*,\lambda_1^*,t)$ is the corresponding Routhian function. We also have the boundary conditions on λ_2,

$$\lambda_2^*(t_0)=\frac{\partial\phi^*}{\partial p_a(t_0)}+\frac{\partial H^*}{\partial\dot{p}_a}(t_0), \tag{14}$$

$$\lambda_2^*(t_f)=-\frac{\partial\phi^*}{\partial p_a(t_f)}+\frac{\partial H^*}{\partial\dot{p}_a}(t_f). \tag{15}$$

Considering the Hamiltonian in Eq. (9), its partial derivative with respect to $\dot{p}_a$ is given by

$$\frac{\partial H}{\partial\dot{p}_a}(t)=-\frac{kT[n_T-n_l(t)][p_a(t)-p_g^\infty]}{p_a^2(t)}+\lambda_2(t). \tag{16}$$

Thus, by substituting Eq. (16) in Eqs. (14) and (15) and considering the initial and final times t_0 and t_f, the boundary conditions in Eqs. (14) and (15) simplify to

$$\frac{\partial\phi^*}{\partial p_a(t_0)}=\frac{kT(n_T-n_l^0)[p_a^*(t_0)-p_g^\infty]}{(p_a^*)^2(t_0)}, \tag{17}$$

$$\frac{\partial\phi^*}{\partial p_a(t_f)}=-\frac{kT(n_T-n_l^f)[p_a^*(t_f)-p_g^\infty]}{(p_a^*)^2(t_f)}. \tag{18}$$

These derivatives can be integrated to yield the initial and final costs associated with an initial and final pressure different from p_g^∞. In the case of a full first-order phase transition, the final cost will not depend on the final pressure since the total number of molecules of the system is transferred to the liquid phase, $n_l^f=n_T$. In this case, we have no final cost since the process is completely done and the final pressure value at τ is irrelevant as far as the excess work is concerned. However, we would like the initial applied pressure to be equal to p_g^∞. By integrating Eq. (17), we get

$$\phi^*(p_a(t_0))=kT(n_T-n_l^0)\left(\ln\frac{p_a^*(t_0)}{p_g^\infty}-\frac{[p_a^*(t_0)-p_g^\infty]}{p_a^*(t_0)}\right). \tag{19}$$

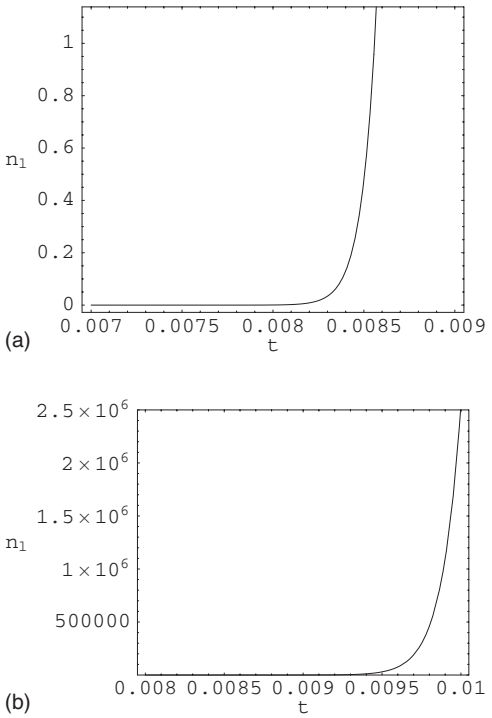

FIG. 2. Number of molecules n_l of nitrogen in the liquid phase due to nucleation in the time interval $0\leq t\leq t_0$ with $t_0=0.01$ s.

TABLE II. The number of critical clusters, the optimal number of molecules both in the liquid phase and per critical cluster, and the critical size at time $t_0=0.01$ for nitrogen N_2.

τ	$N^c(t_0)$	$n_l^*(t_0)$	$n_l^*(t_0)/N^c(t_0)$	$n_l^c(t_0)$
1	5.01897×10^8	6.11503×10^{10}	122	118
10	1.57272×10^7	2.11668×10^9	135	130
10^2	496830	7.34058×10^7	148	144
10^3	15782	2.54588×10^6	161	157
10^4	499	87563	175	171
10^5	16	3006	190	185

These considerations have some practical implications regarding the implementation of the algorithm presented in the next section.

C. Algorithm

Due to the complexity of the Routhian function, the algorithm is composed of the following steps.

Step 1. Consider expression (13), $[(d/dt)(\partial\tilde{H}/\partial\dot{p}_a)-\partial\tilde{H}/\partial p_a](n_l^*,p_a^*,\dot{n}_l^*,\lambda_1^*,t)=0$, and solve it for $\lambda_1^*=\lambda_1(n_l^*,p_a^*,\dot{n}_l^*,t)$. Find $\dot{\lambda}_1^*=\dot{\lambda}_1(n_l^*,p_a^*,\dot{n}_l^*,\dot{p}_a^*,\ddot{n}_l^*,t)$.

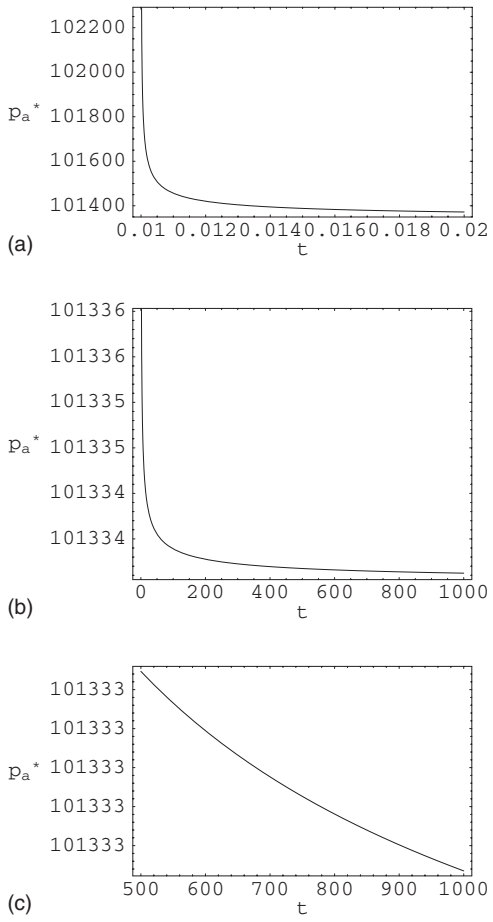

FIG. 3. Optimal applied pressure $p_a^*(t)$ with final time $\tau=10^3$ s for nitrogen N_2.

TABLE III. The initial pressure $p_a^*(t_0)$, the final pressure $p_a^*(\tau)$, and the total excess work performed within time τ for nitrogen N_2.

τ (s)	$p_a^*(t_0)$ (Pa)	$p_a^*(\tau)$ (Pa)	ΔW_{exc} (J)
1	228415	101337	3.233
10	222330	101334	3.221
10^2	216955	101333	3.205
10^3	212165	101333	3.194
10^4	207855	101333	3.187
10^5	203960	101333	3.180

Step 2. Use expression (10) and its derivative with respect to t and substitute them in both λ_1^* and $\dot{\lambda}_1^*$. Since $\dot{n}_l^*=\dot{n}_l(n_l^*,p_a^*,t)$, the adjoint variable and its derivative become $\lambda_1^*=\lambda_1(n_l^*,p_a^*,t)$ and $\dot{\lambda}_1^*=\dot{\lambda}_1(n_l^*,p_a^*,\dot{p}_a^*,t)$.

Step 3. Substitute λ_1^* and $\dot{\lambda}_1^*$ from step 2 into expression (12), $(\dot{\lambda}_1+\partial\tilde{H}/\partial n_l)(n_l^*,p_a^*,\dot{p}_a^*,\lambda_1^*,\dot{\lambda}_1^*,t)=0$, and solve for $\dot{p}_a^*$. We obtain $\dot{p}_a^*=\dot{p}_a(n_l^*,p_a^*,t)$.

Solving the optimal control problem has thus been reduced to numerically solving the following system of differential equations:

$$\dot{p}_a^*=\dot{p}_a(n_l^*,p_a^*,t),\quad \dot{n}_l^*=\dot{n}_l(n_l^*,p_a^*,t)=\frac{\partial\tilde{H}^*}{\partial\lambda_1},$$

$$p_a^*(t_0)=p_a^0,\quad n_l^*(t_0)=n_l^0, \tag{20}$$

in which the last term is obtained by integrating the nucleation term of Eq. (2),

$$n_l^*(t_0)=\int_0^{t_0} n_l^c J_{ss}^c dt, \tag{21}$$

after inserting the linear function $p_a(t)=\{[p_a^*(t_0)-p_g^\infty]/t_0\}t+p_g^\infty$ and considering $n_l^*(0)=0$.

The final optimal state, $n_l^*(\tau)=n_T$ at $t=\tau$, is embedded in the model. We shall now implement the algorithm by first fixing the final time $t_f=\tau$, and then choosing the initial pressure $p_a(t_0)$ such that $n_l(\tau)=n_T$ and W_{exc} is a minimum. The initial pressure $p_a(t_0)$ is the tool we necessarily need to complete the transition process in a fixed time and to minimize the excess work. It is evident that smaller values of t_f require

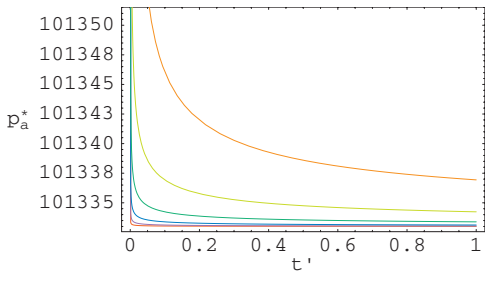

FIG. 4. (Color) Optimal applied pressures $p_a^*(t')$ vs t' in units of pascals for nitrogen N_2. $\tau=1$, orange; 10, light green; 10^2, green; 10^3, blue; 10^4, purple; 10^5, red.

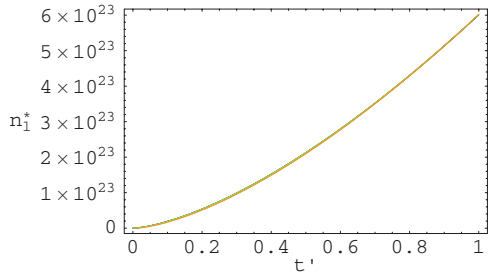

FIG. 5. (Color) Optimal molecule transfer's trajectory $n_l^*(t')$ vs t' for nitrogen N_2. For notation see Fig. 4.

higher initial pressures. But, due to experimental motivation, we would like to start the transition process from the gas to the liquid phase at the standard pressure p_g^∞. It turns out that this apparent drawback can be solved in a natural way as part of the numerical integration of the differential equations. Indeed, we cannot really start our numerical calculations with an initial time $t_0=0$ due to technical computational difficulties. So our strategy is to set the initial time $t_0>0$ (e.g., $t_0=0.01$), assume that in the interval $0\leq t\leq t_0$ the pressure is linearly increased from p_g^∞ to $p_a(t_0)$, apply the algorithm to find the optimal solution (n_l^*, p_a^*) in the interval $t_0\leq t\leq\tau$, and include the initial cost into the minimum total excess work cost obtained along the optimal trajectories. At this point, the pressure has reached some optimal value, i.e., $p_a^*(\tau)=p_a^\tau$, and all the molecules available in the system are in the liquid phase. We can now reduce the applied pressure down to p_g^∞ in any fashion, since no gas phase remains and, thus, W_{exc} does not change.

Let us now apply our formalism to three concrete examples, the liquification of three gases: the two main components of the atmosphere by volume, nitrogen and oxygen, which, together, comprise most of the dry atmosphere, and water vapor.

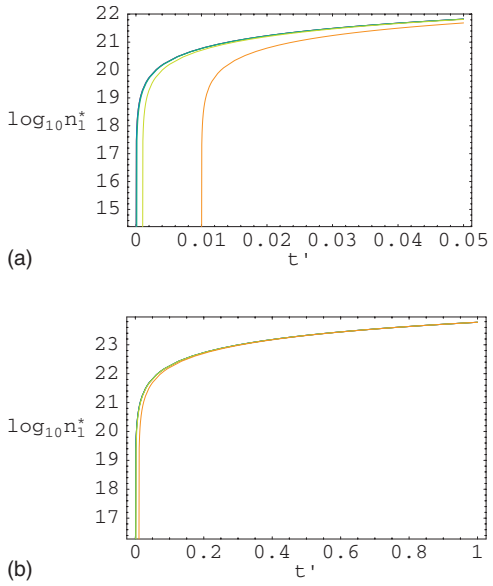

FIG. 6. (Color) $\log_{10} n_l^*(t')$ for nitrogen N_2. For notation see Fig. 4.

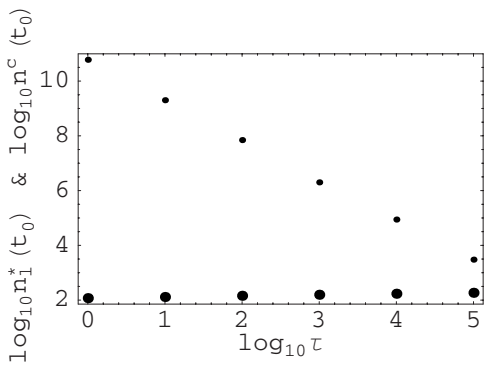

FIG. 7. $\log_{10} n_l^*(t_0)$ (small dots) and $\log_{10} n_l^c(t_0)$ (big dots) vs $\log_{10}\tau$ for nitrogen N_2. The corresponding slopes are $s\approx-1.46$ and $s\approx0.04$.

IV. APPLICATIONS

In the following three examples, we show the optimal trajectories of the applied pressure $p_a^*(t)$ and of the number of molecules in the liquid phase $n_l^*(t)$, for six different fixed final times $\tau=10^5, 10^4, 10^3, 10^2, 10, 1$, in seconds. We shall begin with nitrogen N_2, then present results for oxygen O_2, and finally water vapor H_2O.

Example 1: Nitrogen (N_2). Consider the case of one mole of nitrogen at the boiling temperature $T=T^{boil}=77.355$ K at $p_g=p_g^\infty=1$ atm with the corresponding parameters given in Table I. We shall discuss the case of the first-order phase transition to be completed within the time $\tau=10^3$ as an example in detail; due to the general similarity of the trajectories for the remaining τ's, even though different values of pressure and excess work are obtained. We shall then consider all six cases together and discuss their features.

Given a fixed $\tau=10^3$ and initial time $t=t_0=0.01$ s, the optimal initial applied pressure is $p_a^*(t_0)\approx212165$ Pa, with an initial number of molecules already transferred to the liquid phase of $n_l^*(t_0)\approx2.55\times10^6$. Indeed, during the linear path of the applied pressure in the interval $0\leq t\leq t_0$, the number of molecules transferred to the liquid phase is very small at first [see Fig. 2(a)], but picks up extremely quickly close to t_0 [Fig. 2(b)].

We recall that the linear applied pressure behavior is an assumption reasonable to make to reach the initial optimal pressure value $p_a^*(t_0)$, the starting point of the optimal pressure trajectory.[4] It is interesting to note that, for the $\tau=10^3$ case under investigation, the number of critical clusters created in the time interval $0\leq t\leq t_0$ is about 15 782 (see Table II). This feature of a big growth in the number of critical clusters in the first part of the total pressure path with essentially no contribution along the subsequent optimal trajectory is common for all times τ. Once we have reached the optimal initial applied pressure $p_a^*(t_0)$, the pressure path drops down extremely fast within a fraction of a second [see Fig. 3(a)], and then follows the trajectory shown in Fig. 3(b), which gives a better idea of its very slowly decreasing behavior after the initial drop. Figure 3(c), on the other hand, shows

[4]Of course, the dependence of the results on the choice of t_0 will be investigated in the discussion.

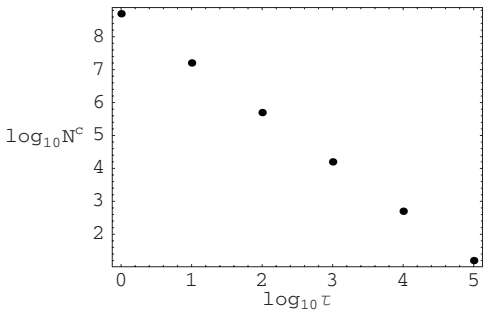

FIG. 8. $\log_{10} N^c$ vs $\log_{10} \tau$ for nitrogen N_2. The slope is $s \approx -1.5$.

the behavior of p_a^* at the end of the transition process, reaching $p_a^*(10^3) = 101\ 333$ Pa. For the interval $[t_0, 10^3]$, we find a negative excess work due to the rapidly decreasing optimal pressure path $W_{exc}(10^3) - W_{exc}(t_0) \approx -136.094$ J, to which we need to add the initial cost $W_{exc}(p_a^*(t_0)) \approx 139.288$ J. In other words, while in the first stage of the process we do work to supersaturate the gas up to $p_a^*(t_0)$, in the second stage we regain most of the work spent. Thus, the total minimum excess work obtained along the entire process is $W_{exc} \approx 3.194$ J. Corresponding results are obtained for the other five values of τ (see Table III). By rescaling the six trajectories in such a way that the applied pressure is a function of $t' = t/\tau$, we show in Fig. 4 all the different pressure paths. In particular, we see that the optimal pressure trajectories shift downward as the final time τ increases. At this point, it is worth mentioning that the initial optimal pressure decreases slightly with increasing τ.

Along the optimal applied pressure paths $p_a^*(t')$ for all six values of τ, the optimal trajectories n_l^* are also very similar throughout the time interval, Fig. 5, except at the beginning. To visualize this point in a clearer way, let us consider the plot $\log_{10} n_l^*$ vs t', in which the six trajectories start at different values t' due to the rescaling [see Fig. 6(a)], and merge rather quickly as is shown in Fig. 6(b).

The number of molecules migrated to the liquid phase at $t = t_0$ is given in Table II, and we represent them as the smaller dots in Fig. 7.

Next, we estimate the number of molecules per critical cluster due only to the nucleation process that essentially takes place within the time interval $[0, t_0]$. To do so, we consider the number of clusters created and the number of molecules already in the liquid phase within $t = t_0$ given in Table II.[5] In all cases, $n_l^*(t_0) \ll n_T \approx 6 \times 10^{23}$. Results are given in Table II.

Most of the molecule transfer happens rather quickly via creation of new clusters of critical size (see Table II), and then tends to stabilize at a much slower rate where growth of the individual clusters is dominant. We show the relation between the number of critical clusters with respect to τ in Fig. 8.

[5]Note that the reason why the critical size n_l^c at $t = t_0$ in Table II has lower values than the number of molecules per cluster given by the ratio n_l^*/N^c is due to the fact that n_l^c is evaluated exactly at the initial optimal pressure p_a^* at t_0, Eq. (A3), while the ratio is an average along the linear path $[p_g^\infty, p_a^*]$.

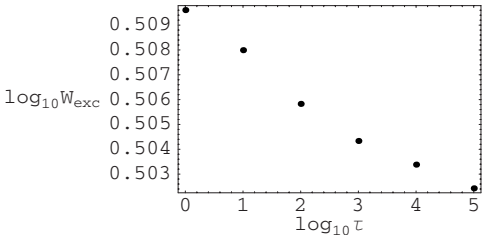

FIG. 9. $\log_{10} W_{exc}$ vs $\log_{10} \tau$ for nitrogen N_2. The slope is $s \approx -0.001\ 436$.

Table III shows, for given τ, the initial pressure $p_a^*(t_0)$, the final pressure $p_a^*(\tau)$, and the total excess work performed to achieve the first-order phase transition within time τ. The difference in initial pressures between the smallest and the biggest values of τ we have considered, $\tau = 1$ and 10^5 s, is around 0.24 atm with a difference in total excess work $W_{exc}^1 - W_{exc}^{10^5} = 0.053$ J.

It is interesting to consider a log-log plot of the excess work W_{exc} vs the available time τ (see Fig. 9). The six points in Fig. 9 lie on essentially a straight line, whose slope is $s \approx -0.001\ 436$.

In Fig. 10, we finally show the initial optimal pressure value obtained vs the available time τ.

Example 2: Oxygen (O_2). Consider the case of one mole of oxygen at the boiling temperature $T = T^{boil} = 90.15$ K at $p_g = p_g^\infty = 1$ atm with the corresponding parameters given in Table I. Considering again the case $\tau = 10^3$, the optimal initial pressure found is $p_a^*(t_0) \approx 238\ 365$ Pa with an initial number of molecules transferred within $t = t_0$ of about $n_l^*(t_0) \approx 2.87 \times 10^6$. Again, only a small growth of n_l is observed at first, followed by a rapid increase to the value given above at $t = t_0$. Moreover, the optimal pressure path follows the behavior plotted in Fig. 3, even though the pressure values at each instant of time are higher than for nitrogen. The final optimal pressure is given by $p_a^*(10^3) \approx 101\ 333$ Pa, with an excess work $W_{exc}(10^3) - W_{exc}(t_0) \approx -204.893$ J, to which we need to add the initial cost $W_{exc}(p_a^*(t_0)) \approx 210.255$ J. Therefore, the total minimum excess work obtained along the entire path for $\tau = 10^3$ is $W_{exc} \approx 5.362$ J. Detailed results for the oxygen case are given in Table V below. Figure 11 shows all the pressure paths as functions of $t' = t/\tau$.

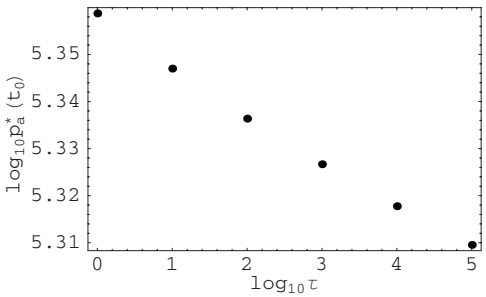

FIG. 10. $\log_{10} p_a^*(t_0)$ vs $\log_{10} \tau$ for nitrogen N_2: $p_a^*(t_0) \propto \tau^{-0.0098}$.

TABLE IV. The number of critical clusters, the optimal number of molecules both in the liquid phase and per critical cluster, and the critical size at time $t_0=0.01$ for oxygen O_2.

τ	$N^c(t_0)$	$n_l^*(t_0)$	$n_l^*(t_0)/N^c(t_0)$	$n_l^c(t_0)$
1	6.58868×10^8	6.88593×10^{10}	104	101
10	2.0628×10^7	2.38264×10^9	115	112
10^2	654592	8.30286×10^7	127	124
10^3	20734	2.87275×10^6	139	135
10^4	658	99161	151	147
10^5	21	3398	163	159

Similarly, the time evolution of $n_l^*(t)$, the number of molecules of oxygen transferred to the liquid phase, shows the same behavior as in the case of nitrogen. The number of molecules migrated to the liquid phase at $t=t_0$ is given in Table IV. Again, both $n_l^*(t_0)$ and $N^c(t_0)$ follow approximately a power law as a function of τ, $n_l^*(t_0)\propto\tau^{-1.46}$ and $N^c\propto\tau^{-1.5}$. As is evident from Table IV, within a very small time frame a considerable amount of molecules migrates to the liquid phase due to nucleation.

Table V shows for given τ the following quantities: the initial pressure $p_a^*(t_0)$, the final pressure $p_a^*(\tau)$, and the total excess work needed to achieve the first-order phase transition within time τ. The difference in initial pressures between the smallest and the biggest values of τ we have considered, $\tau=1$ and 10^5 s, is bigger than for the nitrogen case (about 0.32 atm), with a difference in total excess work $W_{exc}^1-W_{exc}^{10^5}=0.097$ J. When we consider the relation between the excess work W_{exc} and the final time τ given in Fig. 12, we note that, in the case of oxygen, the slope of the line connecting the six points in Fig. 12 is essentially identical to the nitrogen one, namely, $s\approx-0.001\,566$.

Finally, the initial optimal pressure value as function of the available time τ also exhibits a power law given by $p_a^*(t_0)\propto\tau^{-0.0114}$.

Example 3: Water vapor (H_2O). For the case of the first-order phase transition of one mole of water vapor at the boiling temperature $T=T^{boil}=373.15$ K at $p_g=p_g^\infty=1$ atm to the liquid phase within the time $\tau=10^3$ s (the corresponding parameters are given in Table I), we find an optimal initial pressure $p_a^*(t_0)\approx202\,335$ Pa, with an initial number of molecules given by $n_l^*(t_0)\approx1.23\times10^7$. The final optimal pressure is given by $p_a^*(10^3)\approx101\,333$ Pa, with an excess work

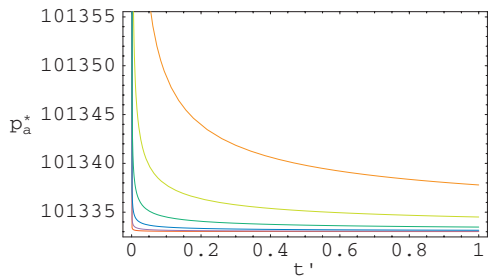

FIG. 11. (Color) Optimal applied pressures $p_a^*(t')$ vs t' in pascals for oxygen O_2. For notation see Fig. 4.

TABLE V. The initial pressure $p_a^*(t_0)$, the final pressure $p_a^*(\tau)$, and the total excess work performed within time τ for oxygen O_2.

τ (s)	$p_a^*(t_0)$ (Pa)	$p_a^*(\tau)$ (Pa)	ΔW_{exc} (J)
1	259730	101338	5.430
10	251695	101335	5.407
10^2	244640	101333	5.380
10^3	238365	101333	5.362
10^4	232750	101333	5.346
10^5	227685	101333	5.333

$W_{exc}(10^3)-W_{exc}(t_0)\approx-561.389$ J, to which we need to add the initial cost $W_{exc}(p_a^*(t_0))\approx596.714$ J. Thus, the total minimum excess work obtained along the optimal solution (n_l^*,p_a^*) is $W_{exc}\approx35.325$ J.

Again, by rescaling the six trajectories in such a way that the applied pressure is a function of $t'=t/\tau$, we find that all the pressure paths are very similar (see Fig. 13).

The functions n_l^* for all the six times τ are also again very similar throughout the time interval except at the very beginning. The number of molecules transferred to the liquid phase at $t=t_0$ is given in Table VI, and we again find a power-law behavior for $n_l^*(t_0)\propto\tau^{-1.46}$, $n^c(t_0)\propto\tau^{0.04}$, and $N^c\propto\tau^{-1.5}$.

In Table VII, we list for a given τ the initial pressure $p_a^*(t_0)$, the final pressure $p_a^*(\tau)$, and the total excess work done to achieve the first-order phase transition within time τ. The difference in initial pressures between the smallest and the biggest values of τ we have considered, $\tau=1$ and 10^5 s, is about 0.23 atm, with a relatively big difference in total excess work $W_{exc}^1-W_{exc}^{10^5}=0.836$ J, compared to N_2 and O_2.

In Fig. 14, we show the log-log plot of the excess work W_{exc} vs the time τ with the slope of the line connecting the points given by $s\approx-0.002\,046$. This is quite similar to the value found for nitrogen and oxygen.

Finally, the initial optimal pressure value obtained with respect to the available time τ exhibits a power-law dependence $p_a^*(t_0)\propto\tau^{-0.0096}$.

V. DISCUSSION

A. Aspects of the gas-liquid phase transition

The three examples we have investigated present similarities and differences that are worth discussing. We have no-

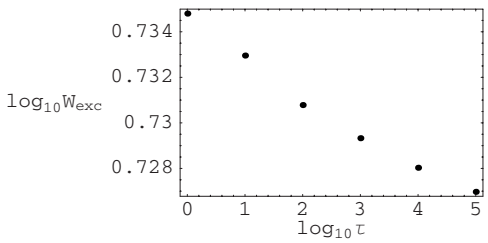

FIG. 12. $\log_{10}W_{exc}$ vs $\log_{10}\tau$ for oxygen O_2. The slope is $s\approx-0.001\,566$.

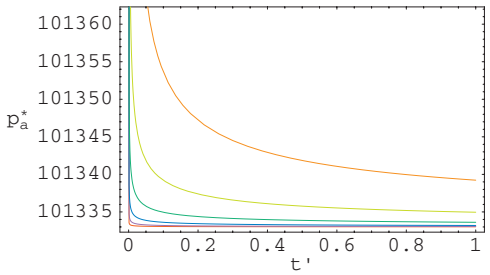

FIG. 13. (Color) Optimal applied pressures $p_a^*(t')$ vs t' for water vapor H_2O. For notation see Fig. 4.

ticed throughout the previous section how the behaviors of the optimal applied pressure paths, $p_a^*(t)$, in the time interval $[t_0,\tau]$, are similar within the same system for different τ's (see Figs. 4, 11, and 13), and for the same τ for different systems (see Fig. 15). This is due to the fact that, after a first increase in pressure with corresponding excess work spent and molecules transferred to the liquid phase along a linear trajectory, there is a relaxation of the applied pressure needed to minimize the excess work along the optimal path.

The power law relating the initial applied pressure $p_a^*(t_0)$ for the three systems is given in Table VIII and is shown in Fig. 16(a). It is evident how the initial optimal pressure $p_a^*(t_0)$ decreases with increasing τ for the three systems. The actual value of $p_a^*(t_0)$ is due to the complicated interplay of surface tension, boiling temperature, and molecular volume in Eqs. (A3) and (A4). We find that for $T=T_{boil}$ ($p_g^\infty=1$ atm) the oxygen system requires higher pressure values at $T=T_0$, followed by nitrogen and water vapor, but no simple formula appears to be available to predict this sequence.

For the initial time interval $[0,t_0]$ where the very rapid initial increase in pressure takes place, we recall that the applied pressure path is identical for all situations, since we have assumed a linear growth from the transition pressure p_g^∞ to $p_a^*(t_0)$. It is interesting to note that, along this first part of the pressure trajectory, the number of molecules transferred to the liquid phase due to nucleation is very similar for the three systems [see Fig. 16(b)]. Specifically, it is slightly greater for water vapor followed by oxygen and nitrogen. This behavior is due to lower pressure values at t_0 [see Fig. 16(a)], which imply higher critical sizes [see Fig. 17(a)], and to a higher number of critical clusters created within $0\leq t\leq t_0$ [see Fig. 17(b)]. The power laws for $n_l^*(t_0)$, $n_l^c(t_0)$, and $N^c(t_0)$ are given in Table VIII, exibiting very similar behavior. Regarding the relation between the excess work W_{exc} as the energy spent in supersaturating the system and the time τ available, we also observe a power law, given in Table VIII. It is found that water vapor requires a much greater amount of excess work to supersaturate the gas compared to oxygen and nitrogen, even though the optimal pressure path for water vapor has lower values than the other two systems. This fact implies that the change in volume throughout the phase transition has to be greater for water vapor than for the other two gases. Indeed, when we analyze Eq. (3) we notice how higher temperature values, on the one hand, and lower pressure values, on the other, determine the volume change throughout the process, with a pressure rate and molecule transfer rate essentially similar for the three systems at given τ. Our results strongly suggest that systems with higher (optimal) pressure and lower temperature values will probably require the least amount of excess work to achieve a change of phase. Another important technical point that needs to be addressed is the relevance of the choice of the initial time t_0 and of the choice of a linear increase of the applied pressure in the time interval $[0,t_0]$ as far as the excess work is concerned. We find for all three examples that the choice of t_0 and the behavior of $p_a^*(t)$ in $[0,t_0]$ are essentially irrelevant as long as we do not force the system to remain for a long time at the peak value $p_a^*(t_0)$—in this case, the excess work increases considerably and $p_a^*(t)$ is clearly no longer an optimal path. For simplicity we shall present the results for only one instance. Supposing we have $\tau=10^3$ s available for the gas-liquid phase transition of nitrogen N_2, let us set $t_0=0.0001$, 0.005, 0.02 s besides the already investigated case of $t_0=0.01$ s. In Table IX, it is shown that the total excess work spent along the entire trajectory within the time

TABLE VI. The number of critical clusters, the optimal number of molecules both in the liquid phase and per critical cluster, and the critical size at time $t_0=0.01$ for water vapor H_2O.

τ	$N^c(t_0)$	$n_l^*(t_0)$	$n_l^*(t_0)/N^c(t_0)$	$n_l^c(t_0)$
1	2.37112×10^9	2.91248×10^{11}	123	119
10	7.42602×10^7	1.01291×10^{10}	136	132
10^2	2.35108×10^6	3.5365×10^8	150	146
10^3	74522	1.22897×10^7	165	161
10^4	2361	424752	180	175
10^5	75	14614	195	191

TABLE VII. The initial pressure $p_a^*(t_0)$, the final pressure $p_a^*(\tau)$, and the total excess work performed within time τ for water vapor H_2O.

τ (s)	$p_a^*(t_0)$ (Pa)	$p_a^*(\tau)$ (Pa)	ΔW_{exc} (J)
1	217600	101339	35.90
10	211860	101335	35.684
10^2	206817	101334	35.480
10^3	202335	101333	35.325
10^4	198320	101333	35.190
10^5	194700	101333	35.064

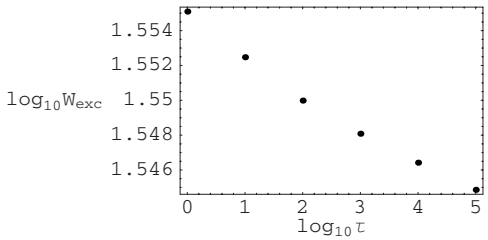

FIG. 14. $\log_{10} W_{exc}$ vs $\log_{10}\tau$ for water vapor H_2O. The slope is $s\approx-0.002\,046$.

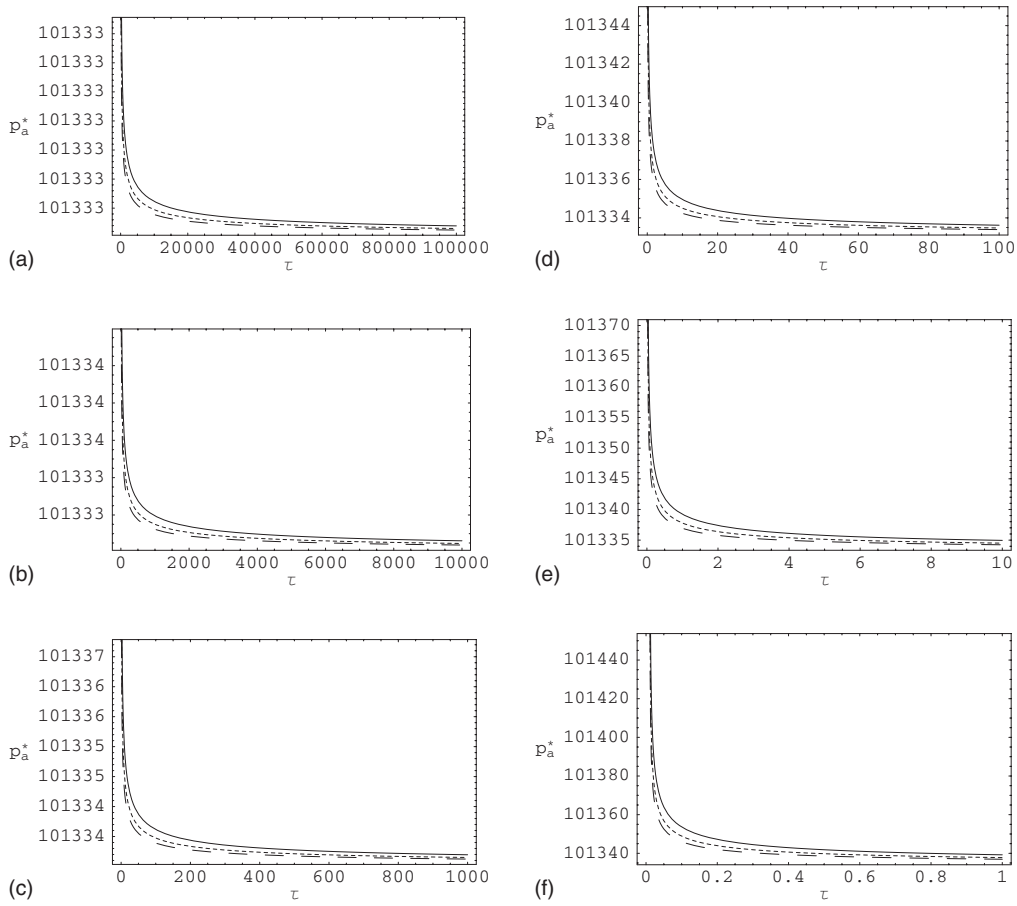

FIG. 15. Optimal applied pressure paths $p_a^*(t)$ for oxygen O_2 (dotted line), nitrogen N_2 (dashed line), and water vapor H_2O (full line) with different final times τ.

interval $[0,\tau]$ is essentially invariant with respect to the initial time chosen t_0. The reason is that the minimal increase of excess work along the optimal pressure path p_a^* as t_0 increases is counterbalanced by a decrease in the initial cost $W_{exc}(p_a^*(t_0))$.

It is important to stress that this work represents a first approach in analyzing a first-order phase transition in a closed system using methods and objectives from finite-time thermodynamics. Thus, the choice of classical nucleation theory as the main framework for the creation and growth of clusters, and the consideration of only critical clusters, have to be seen as a first attempt to put together different fields such as nucleation theory, finite-time thermodynamics, and optimal control theory. Nevertheless, the authors are aware that the kinetics of nucleation is a multistage process in which the evolution of clusters in cluster size space is dominated by different factors depending on the size. Indeed, the evolution of a cluster of size greater than $n_l^c+\delta n_l^c$ is domi-

TABLE VIII. Power laws of $n_l^*(t_0)$, $n_l^c(t_0)$, N_l^c, $p_a^*(t_0)$, and W_{exc} as a function of τ for nitrogen, oxygen, and water vapor.

	Nitrogen	Oxygen	Water vapor
$n_l^*(t_0)$	$6.11\times10^{10}\tau^{-1.46}$	$6.88\times10^{10}\tau^{-1.46}$	$2.91\times10^{11}\tau^{-1.46}$
$n_l^c(t_0)$	$118\tau^{0.04}$	$101\tau^{0.04}$	$119\tau^{0.04}$
N_l^c	$5.02\times10^{8}\tau^{-1.5}$	$6.59\times10^{8}\tau^{-1.5}$	$2.37\times10^{9}\tau^{-1.5}$
$p_a^*(t_0)$	$228415\tau^{-0.0098}$	$259730\tau^{-0.0114}$	$217600\tau^{-0.0096}$
W_{exc}	$3.233\tau^{-0.001436}$	$5.43\tau^{-0.001566}$	$35.9\tau^{-0.002046}$

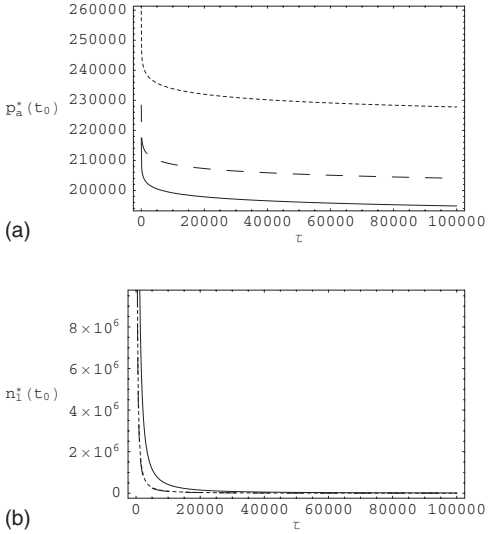

FIG. 16. (a),(b) Power laws as function of τ for $p_a^*(t_0)$ and $n_l^*(t_0)$ as listed in Table VIII. For notation see Fig. 15.

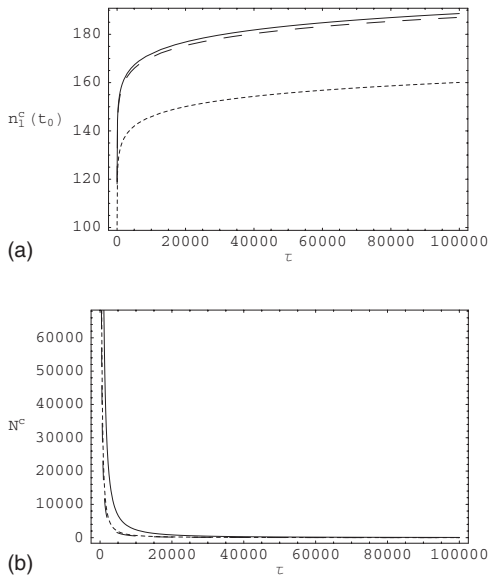

FIG. 17. (a),(b) Power laws as function of τ for $n_l^c(t_0)$ and N^c as listed in Table VIII. For notation see Fig. 15.

nated by the deterministic growth term in the Frenkel-Zeldovich equation, and not by a diffusionlike process as in the interval in cluster size space $(n_l^c-\delta n_l^c, n_l^c+\delta n_l^c)$, or by a stochastic process as below $n_l^c-\delta n_l^c$ [20,21]. Clearly, any model can be improved, and it is our goal to extend our approach to the nonisothermal case in which creation and growth of clusters of different sizes are considered and in which non-steady-state effects in the intial stage of the nucleation process are introduced [20,21]. Moreover, in our work we consider closed systems which undergo a change in volume during the phase transition. This implies that, as molecules condense into clusters of critical sizes and vapor consumption during the process is achieved, we still retain quasi-steady-state conditions due to the decrease in volume of the system. Such a picture is different from the classical Szilard model [20,21] which deals with systems in which the nuclei reaching supercritical size are removed from the system and reintroduced as monomers so as to keep a certain fixed degree of supersaturation.

The results obtained in this paper could be extremely useful, in our opinion, for applied and experimental work, and further studies on controlling first-order gas-liquid phase transitions in a finite time. One needs to keep in mind, however, that in the homogeneous nucleation theory the vapor phase is supposed to behave as an ideal gas and therefore the excess work values obtained in this paper might be considered as upper bounds for real systems. These bounds have to be attributed to the fact that in real systems attractive forces are present among the molecules, facilitating the condensation of molecules to the clusters and, thus, requiring less work to supersaturate the gas and to obtain the phase transition. Furthermore, one also needs to take into account the simplifications of avoiding evaporation of clusters throughout the process and avoiding coarsening behaviors when judging the quantitative accuracy of the results obtained with respect to the excess work during the phase transition in real applications. We are going to investigate this issue in future work and compare with our present results; however the technical difficulties in numerical computations are quite large. Similarly, the issue of heat flux between the clusters of the new phase and the old phase and the question of internal relaxations to equilibrium upon changes of the control parameters could also be addressed in future work. If we look at our work as a starting point in studying the general gas-liquid first-order phase transition in the context of finite-time thermodynamics and optimal control theory, a first step in the direction of a more complete study might be to consider a nonisothermal homogeneous nucleation reaction combined with a backward molecular transfer rate for a gas-liquid transition [13,22]. In this case, the change in energy upon condensation, $\Delta H=H_{vap}-H_{liq}$, is always positive, but we note that it might have either sign in, e.g., solid-solid phase transitions. Therefore, the change in energy due to the gain or loss of a monomer from a cluster is given by $E=\Delta H-W$, where W is the work needed to increase the area of the interface [22].

B. Applicability to general first-order phase transitions

To what extent is the approach we have presented for the example of the gas-liquid transition applicable to a general first-order phase transition? Central elements of our analysis were a nucleation rate, a growth rate, an excess work rate, the set of state and control parameters, and finally the optimal control problem. Quite generally, a first-order phase transition often begins with a nucleation process and subsequent growth of the size of the nuclei with time, and, at the end of the process, a new phase is formed. Assuming spherical nuclei of radius r (or some other size parameter), the total variation of the Gibbs free energy ΔG is classically given by

$$\Delta G = \Delta H - T\Delta S, \tag{22}$$

where $\Delta H=N^r\Delta G_{nucl}^r$ is the enthalpy associated with the formation through nucleation of clusters of radius r. ΔG_{nucl}^r is the Gibbs energy associated with the formation of a cluster

TABLE IX. The initial pressure p_a^*, the critical size n^c, the number of critical clusters N^c, and the excess work ΔW_{exc} with $\tau=10^3$ s for the gas-liquid phase transition of nitrogen N_2 for different values of t_0.

t_0	$p_a^*(t_0)$	$n^c(t_0)$	$N^c(t_0)$	$W_{exc}(p_a^*(t_0))$	ΔW_{exc} $(t_0\le t\le\tau)$	ΔW_{exc} $(0\le t\le\tau)$
0.0001	218675	140	15693	149.581	−146.375	3.206
0.005	213085	155	15770	140.745	−137.549	3.196
0.01	212165	157	15782	139.288	−136.094	3.194
0.02	211265	160	15801	137.863	−134.669	3.194

of radius r, which includes a term corresponding to the passage of molecules from one phase to the other and a term corresponding to the creation of an interface between the cluster of the new phase and the initial phase [1]. Moreover, ΔS is the variation of the entropy associated with the formation of N^r nuclei of radius r in the parent phase. Thus, rewriting the total variation of the Gibbs energy as $\Delta G = N^r \Delta G^r_{nucl} - T\Delta S$, the value of N^r corresponding to equilibrium satisfies the relation

$$\frac{\partial \Delta G}{\partial N^r} = 0. \tag{23}$$

The nucleation rate is, in general, defined by the relation,

$$J = \frac{dN}{dt} = b^c N_s^0 N^c, \tag{24}$$

where $N(t)$ is the number of nuclei formed in the system at time t, b^c is the rate of collision of molecules with the critical clusters, N^c is the number of nuclei of critical size r^c, and N_s^0 is the number of molecules on the surface of a nucleus [1]. Of course, depending on the type of phase transition, an appropriately modified model describing the rate of the state parameters involved in the problem has to be defined. If such a model needs to address a transition between different physical phases, e.g., gas-liquid, liquid-solid, paramagnetic-ferromagnetic, etc., then both a nucleation and a growth term have to be present, completely analogous to our approach. Similarly, we are confident that our approach to optimizing a gas-liquid first-order phase transition in the context of finite-time thermodynamics could be extended to heterogeneous nucleation reactions occurring on foreign surfaces in a supersaturated vapor, possibly with the inclusion of a backward molecule transfer rate. Here, a first step could consist of considering an isothermal heterogeneous nucleation process, still in the gas-liquid regime, where the surface-absorbed monomers have the same temperature and chemical potential as the monomers in the parent phase.

VI. SUMMARY

In this paper, we have studied a first-order phase transition in the context of finite-time thermodynamics and optimal control theory, using the gas-liquid transition as an example. We modeled the molecular transfer from the gas to the liquid phase, within the context of classical homogenoeus nucleation theory, and set up and solved the optimal control problem such that a phase transition of one mole of gas was achieved in a finite time through supersaturation while the work of supersaturating the gas was minimized. Finally, we applied our results to three different gases: nitrogen N_2, oxygen O_2, and water vapor H_2O.

APPENDIX A

1. Theory of classical homogeneous nucleation

Starting from the work of Volmer and Weber [23–25], Becker and Döring [26], and Zeldovich [27], the classical nucleation theory is based on equilibrium statistical mechanics and unimolecular reaction kinetics. By assuming a spherical shape of the clusters of radius r, incompressibility of the liquid phase, and ideal behavior of the gaseous phase, and by considering the number of molecules n in a single spherical droplet given by $n=(4\pi/3\nu_l)r^3$, the reversible work of cluster formation ΔW is given by [13]

$$\Delta W_n = -nkT \ln S + 4\pi\gamma\left(\frac{3\nu_l}{4\pi}\right)^{2/3} n^{2/3}, \tag{A1}$$

where ν_l is the volume of a molecule in the droplet, k is the Boltzmann constant, T is the fixed system temperature, and $S=p_g/p_g^\infty$ is the degree of supersaturation, with p_g^∞ being the transition pressure at the given temperature T in thermodynamical equilibrium. The work of cluster formation takes a maximum value

$$\Delta W_{n^c} = \frac{16\pi\nu_l^2\gamma^3}{3k^2T^2(\ln S)^2} \tag{A2}$$

at $n=n^c$ given by

$$n^c = \frac{32\pi\nu_l^2\gamma^3}{3k^3T^3(\ln S)^3}. \tag{A3}$$

The classical rate of nucleation J_{ss}^c is defined as the number of clusters of critical size n^c per unit volume per unit time, and has been derived by Becker and Döring [26] and by Zeldovich [27]:

$$\frac{dN^c}{dt} = J_{ss}^c = Zb^c N_{eq}^c, \tag{A4}$$

where N^c is the number of clusters of critical size, $N_{eq}^c = (p_g/kT)\exp(-\Delta W_{n^c}/kT)$ is the equilibrium number of clusters of critical size per unit volume of the gas, $Z = \sqrt{[-(1/2\pi kT)(\partial^2 \Delta W_n/\partial n^2)_{n=n^c}]} = (kT(\ln S)^2/8\pi\nu_l\gamma)\sqrt{kT/\gamma}$ is the Zeldovich factor, and $b^c = p_g A_{n^c}/\sqrt{2\pi mkT}$ is the frequency of capture of a monomer by a cluster of critical size. The surface area of the critical droplet is given by $A_{n^c} = (4\pi)^{1/3}(3\nu_l)^{2/3}(n^c)^{2/3}$, and the mass of a molecule is indicated by m. We are assuming that the condensation coefficient is unity [13].

Considering all these factors and that $n_g = n_T - n_l$, we can write the steady-state nucleation rate of the gas as

$$J_{ss}^c = \sqrt{\frac{2\gamma}{\pi m}}\nu_l\left(\frac{p_g}{kT}\right)(n_T - n_l)e^{-16\pi\nu_l^2\gamma^3/3k^3T^3(\ln S)^2}. \tag{A5}$$

APPENDIX B

For a general overview of the calculus of variation and optimal control theory we refer to Refs. [28–30]. The typical problem in optimal control consists in finding a continuously differentiable function $\bar{\boldsymbol{u}}(t)$, $t_0 \le t \le t_f$, to minimize [28]

$$\int_{t_0}^{t_f} \mathfrak{I}(\bar{\boldsymbol{x}}(t), \bar{\boldsymbol{u}}(t), t)dt \tag{B1}$$

subject to conditions on the state and costate variables $\bar{\boldsymbol{x}}(t) \in X \subset R^n$ and $\bar{\boldsymbol{u}}(t) \in U \subset R^m$:

$$\dot{\bar{x}}(t) = \boldsymbol{f}(\bar{x}(t), \bar{u}(t), t), \quad \bar{x}(t_0) = \bar{x}_0. \tag{B2}$$

As long as the optimal solution $(\bar{x}^*(t), \bar{u}^*(t))$ is in the interior of the admissible sets (X, U), with continuous controls everywhere in $[t_0, t_f]$, variational methods can be used to obtain the necessary conditions for optimality [28–30] by minimizing the expression

$$\phi(\bar{x}(t_0), t_0, \bar{x}(t_f), t_f) + \int_{t_0}^{t_f} \Im(\bar{x}(t), \bar{u}(t), t)dt, \tag{B3}$$

where $\phi(\cdot) \in R$ is the initial or terminal cost function subject to the state vector's boundary conditions,

$$\boldsymbol{\psi}(\bar{x}(t_0), t_0, \bar{x}(t_f), t_f) = 0, \tag{B4}$$

where $\boldsymbol{\psi}(\cdot) \in R^k$ for some $k \in R$. Introducing an auxiliary vector of costate variables $\bar{\boldsymbol{\lambda}}(t) \in R^n$ leads to a Hamiltonian function H,

$$H(\bar{x}(t), \bar{u}(t), \bar{\boldsymbol{\lambda}}(t), t) = \bar{\boldsymbol{\lambda}}^T \bar{\boldsymbol{f}}(\bar{x}(t), \bar{u}(t), t) - \Im(\bar{x}(t), \bar{u}(t), t). \tag{B5}$$

The general cost functional to be minimized is then given by:

$$J = \phi(\bar{x}(t_0), t_0, \bar{x}(t_f), t_f) + \boldsymbol{\mu}^T \boldsymbol{\psi}(\bar{x}(t_0), t_0, \bar{x}(t_f), t_f) + \int_{t_0}^{t_f} [\bar{\boldsymbol{\lambda}}^T(t) \dot{\bar{x}}(t) - H(\bar{x}(t), \bar{u}(t), \bar{\boldsymbol{\lambda}}(t), t)]dt, \tag{B6}$$

where $\boldsymbol{\mu}$ is a k-vector of Lagrange multipliers.

The optimal control problem discussed in this work corresponds to the special case in which some state variables are identified as control variables. Our case contains two state variables $x_1 = n_l$ and $x_2 = p_g$, and one control variable $u = p_a$, where $x_2 = u$ since $p_g = p_a$ for all $t \in [t_0, t_f]$ (no time delay). For this case, the minimization leads to the following necessary conditions for the solution of the optimal control problem:

(a) the boundary conditions on the state vector,

$$\boldsymbol{\psi}(\boldsymbol{x}_1^*(t_0), \boldsymbol{u}^*(t_0), t_0, \boldsymbol{x}_1^*(t_f), \boldsymbol{u}^*(t_f), t_f) = 0, \tag{B7}$$

(b) the boundary conditions on the costate vector $\bar{\boldsymbol{\lambda}} = (\boldsymbol{\lambda}_1, \boldsymbol{\lambda}_2)$,

$$(\boldsymbol{\lambda}_1^*)^T(t_0) = \left(\frac{\partial \phi^*}{\partial \boldsymbol{x}_1(t_0)}\right)^T + (\boldsymbol{\mu}^*)^T \frac{\partial \boldsymbol{\psi}^*}{\partial \boldsymbol{x}_1(t_0)},$$

$$(\boldsymbol{\lambda}_2^*)^T(t_0) = \left(\frac{\partial \phi^*}{\partial \boldsymbol{u}(t_0)}\right)^T + (\boldsymbol{\mu}^*)^T \frac{\partial \boldsymbol{\psi}^*}{\partial \boldsymbol{u}(t_0)},$$

$$(\boldsymbol{\lambda}_1^*)^T(t_f) = -\left(\frac{\partial \phi^*}{\partial \boldsymbol{x}_1(t_f)}\right)^T - (\boldsymbol{\mu}^*)^T \frac{\partial \boldsymbol{\psi}^*}{\partial \boldsymbol{x}_1(t_f)},$$

$$(\boldsymbol{\lambda}_2^*)^T(t_f) = -\left(\frac{\partial \phi^*}{\partial \boldsymbol{u}(t_f)}\right)^T - (\boldsymbol{\mu}^*)^T \frac{\partial \boldsymbol{\psi}^*}{\partial \boldsymbol{u}(t_f)}, \tag{B8}$$

(c) the conditions on the Hamiltonian,

$$H_{t_0}^* = -\frac{\partial \phi^*}{\partial t_0} - (\boldsymbol{\mu}^*)^T \frac{\partial \boldsymbol{\psi}^*}{\partial t_0}, \quad H_{t_f}^* = \frac{\partial \phi^*}{\partial t_f} + (\boldsymbol{\mu}^*)^T \frac{\partial \boldsymbol{\psi}^*}{\partial t_f}, \tag{B9}$$

(d) the system dynamic constraint imposed on the problem,

$$\dot{\boldsymbol{x}}_1^* = \frac{\partial H^*}{\partial \boldsymbol{\lambda}_1}, \quad \dot{\boldsymbol{x}}_2^* = \dot{\boldsymbol{u}}^* = \frac{\partial H^*}{\partial \boldsymbol{\lambda}_2}, \tag{B10}$$

(e) the time evolution of the adjoint vector $\bar{\boldsymbol{\lambda}}$,

$$\dot{\boldsymbol{\lambda}}_1^* = -\frac{\partial H^*}{\partial \boldsymbol{x}_1}, \quad \dot{\boldsymbol{\lambda}}_2^* = \frac{d}{dt}\left(\frac{\partial H^*}{\partial \dot{\boldsymbol{u}}}\right) - \frac{\partial H^*}{\partial \boldsymbol{u}}, \tag{B11}$$

and (f) the so-called input stationary function,

$$\frac{\partial H^*}{\partial \boldsymbol{v}} = 0, \tag{B12}$$

with $H^* = H(\boldsymbol{x}_1^*, \boldsymbol{v}^*, \boldsymbol{u}^*, \dot{\boldsymbol{u}}^*, \boldsymbol{\lambda}_1^*, \boldsymbol{\lambda}_2^*, t)$.

[1] P. Papon, J. Leblond, and P. H. E. Meijer, *The Physics of Phase Transitions* (Springer, Berlin, 1999).
[2] D. W. Oxtoby, J. Phys.: Condens. Matter **4**, 7627 (1992).
[3] B. Andresen, M. H. Rubin, and R. S. Berry, J. Phys. Chem. **87**, 2704 (1983).
[4] B. Andresen, R. S. Berry, M. J. Ondrechen, and P. Salamon, Acc. Chem. Res. **17**, 266 (1984).
[5] P. Salamon, J. D. Nulton, G. Siragusa, T. R. Andersen, and A. Limon, Energy **26**, 307 (2001).
[6] J. M. Gordon, I. Rubinstein, and Y. Zarmi, J. Appl. Phys. **67**, 81 (1990).
[7] A. M. Tsirlin, V. A. Mironova, S. A. Amelkin, and V. Kazakov, Phys. Rev. E **58**, 215 (1998).
[8] L. Chen, F. Sun, and C. Wu, J. Phys. D **32**, 99 (1999).
[9] G. Grazzini and R. Rinaldi, Int. J. Therm. Sci. **40**, 173 (2001).
[10] M. Schaller, K. H. Hoffmann, G. Siragusa, P. Salamon, and B. Andresen, Comput. Chem. Eng. **25**, 1537 (2001).
[11] A. Bejan, Appl. Phys. Lett. **79**, 191 (1996).
[12] L. Chen, C. Wu, and F. J. Sun, J. Non-Equilib. Thermodyn. **24**, 27 (1999).
[13] A. C. Zettlemoyer, *Nucleation* (Dekker, New York, 1969).
[14] J. L. Katz, Pure Appl. Chem. **64**, 1661 (1992).
[15] R. Span, E. W. Lemmon, R. T. Jacobsen, W. Wagner, and A. Yokozeki, J. Phys. Chem. Ref. Data **29**, 1361 (2000).
[16] A. A. Kharitonov, *Fluid Dynamics* (Springer,Berlin, 1973).
[17] D. Sonntag and D. Heinze, *Sättigungsdampfdruck und Sättigungsdampfdichtetafeln für Wasser und Eis (Leipzig)* (VEB, Leipzig, 1982).
[18] H. R. Pruppacher and J. D. Klett, *Microphysics of Clouds and Precipitation* (Reidel, Dordrecht, 1980).
[19] S. Lowell and J. E. Shields, *Powder Surface Area and Porosity* (Chapman and Hall, London, 1991).

[20] J. W. P. Schmelzer, G. Röpke, and V. B. Priezzhev, *Nucleation Theory and Applications* (JNR, Dubna, 1999).
[21] J. W. P. Schmelzer, G. Röpke, and V. B. Priezzhev, *Nucleation Theory and Applications* (JNR, Dubna, 2002).
[22] B. E. Wyslouzil and J. H. Seinfeld, J. Chem. Phys. **97**, 2661 (1992).
[23] M. Volmer and A. Weber, Z. Phys. Chem., Stoechiom. Verwandtschaftsl. **119**, 227 (1926).
[24] M. Volmer, Z. Phys. Chem., Stoechiom. Verwandtschaftsl. **25**, 555 (1929).
[25] M. Volmer, *Kinetik der Phasenbildung* (Steinkopff, Dresden, 1939), p. 122.
[26] R. Becker and W. Döring, Ann. Phys. (Leipzig) **416**, 719 (1935).
[27] J. B. Zeldovich, Acta Physicochim. URSS **18**, 1 (1943).
[28] J. Gregory and C. Lin, *Constrained Optimization in the Calculus of Variations and Optimal Control Theory* (Van Nostrand Reinhold, New York, 1992).
[29] E. R. Pinch, *Optimal Control and the Calculus of Variations* (Oxford University Press, Oxford, 1993).
[30] D. E. Kirk, *Optimal Control Theory—An Introduction* (Prentice-Hall, Englewood Cliffs, NJ, 1970).